Article

Orientational Dependence of Linear Dichroism Exemplified by Dyed Spherulites

Jason B. Benedict, John H. Freudenthal, Eva Hollis, and Bart Kahr

J. Am. Chem. Soc., **2008**, 130 (32), 10714-10719 • DOI: 10.1021/ja802322t • Publication Date (Web): 18 July 2008

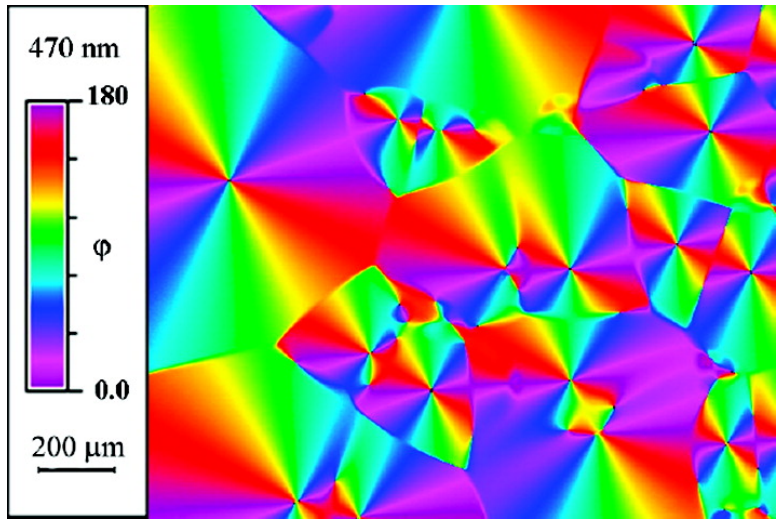

J|A|C|S
ARTICLES

Published on Web 07/18/2008

Orientational Dependence of Linear Dichroism Exemplified by Dyed Spherulites

Jason B. Benedict, John H. Freudenthal, Eva Hollis, and Bart Kahr*

Department of Chemistry, Box 351700, University of Washington, Seattle Washington 98195-1700

Received March 31, 2008; E-mail: kahr@chem.washington.edu

Abstract: D-Sorbitol forms so-called spherulites from under-cooled melts. These polycrystalline formations have optically uniaxial radii. Melts pressed between glasses crystallize as plane sections of spheres. Dyes that are soluble in molten sorbitol become oriented as the crystallization front passes through the melt so as to form disks with large linear dichroism in the absorption bands of the dyes. The dyeing of spherulites is thus a general method of solute alignment. The linear optical properties of sorbitol spherulites containing the azo dye amaranth were analyzed in detail so as to correct a persistent confusion in the literature regarding the orientational dependence of linear dichroism. In cases involving thin film dichroism of multilayered samples requiring many corrections of intensity data in non-normal incidence, some authors have taken transmittance and others absorbance as having a cosine-squared angular dependence on the plane of the electric vector of linearly polarized light. Plane sections of doped spherulites present all orientations of an electric dipole oscillator in spatially localized region in normal incidence. As such, the samples described herein are ideally suited to resolving this confusion. Images of transmittance of dyed spherulites in polarized light were recorded with a CCD camera and simulated under the assumption that both absorbance and transmittance show a cosine-squared angular dependence but with respect to different angles. Transmittance with a cosine-squared dependence follows azimuthal rotations of the spherulite radii around the wave vector, while absorbance with a cosine-squared dependence follows rotations about axes perpendicular to the wave vector, natural consequences of the properties of the optical indicatrix that are often overlooked. Spherulites obviate the substantial experimental complexities that are engendered in non-normal incidence by sample reorientation. Thus, the principles of anisotropic absorption are given in a complete and intuitive fashion.

Introduction

Recently, researchers claimed to have settled confusion in the spectroscopic literature regarding the angular dependence of absorbance (A) and transmittance (T) with respect to incident linearly polarized light.[1] At issue was whether A or T of uniaxial absorbing bodies follows a $\cos^2\theta$ angular dependence on the plane of polarized light. In other words, is eq 1 or eq 2 valid?

$$A(\theta) = A_{\max}\cos^2(\theta) + A_{\min}\sin^2(\theta) \quad (1)$$

$$T(\theta) = T_{\min}\cos^2(\theta) + T_{\max}\sin^2(\theta) \quad (2)$$

We were surprised to discover that such a fundamental question was a source of confusion, especially given authoritative monographs on the subject of linear dichroism (LD).[2] Having ourselves measured the LD of many mixed crystals[3] we were compelled to understand the nature of this confusion and provide a resolution.

The question of the angular dependence of LD arises in the analysis of thin films of membranes,[4] poled polymers,[5] and liquid crystals.[6] The aforementioned research group[1] came down squarely in favor of eq 2 while studying thin films of nematic liquid crystals. They cited the Law of Malus,[7] the first quantitative relationship involving polarized light which states that $I/I_o = T = \cos^2\theta$, where θ is the angle between the plane of linearly polarized light and the preferred direction of a linear analyzer; I/I_o is the fraction of transmitted intensity relative to the incident intensity.

Proper evaluation of systematic errors are critical in measurements of multilayers in non-normal incidence including the following: changes in path length due to Snell's law, the breakdown of Snell's law for extraordinary rays,[8] Fresnel reflection,[9] multiple reflections,[10] changes in area of illumination at oblique angles,[11] and the conicity of the light pencil.[12] A sample ideal for distinguishing between eqs 1 and 2, obviating

(1) Gregoriou, V. G.; Tzavalas, S.; Bollas, S. T. *Appl. Spectrosc.* **2004**, *58*, 655–661.
(2) (a) Michl, J.; Thulstrup, E. W. *Spectroscopy with Polarized Light*; VCH: Weinheim, 1986; (b) Rodger, A.; Nordén, B. *Circular Dichroism and Linear Dichroism*; Oxford University Press: Oxford, 1997.
(3) Kahr, B.; Gurney, R. W. *Chem. Rev.* **2001**, *101*, 893–951.
(4) Johansson, L. B-Å.; Davidsson, Å *J. Chem. Soc., Faraday Trans. I* **1985**, *81*, 1375–1388.
(5) Graf, M. H.; Zobel, O.; East, A. J.; Haarer, D. *J. Appl. Phys.* **1994**, *75*, 3335–3339.
(6) Collings, P. J.; Ratna, B. R.; Shashidhar, R. *Phys. Rev. E* **2003**, *67*, 02175−1-8.
(7) Kahr, B.; Claborn, K. *ChemPhysChem* **2008**, *9*, 43–58.
(8) Hasegawa, T.; Umemura, J.; Takenaka, T. *Appl. Spectrosc.* **1993**, *47*, 338–340.

10.1021/ja802322t CCC: $40.75

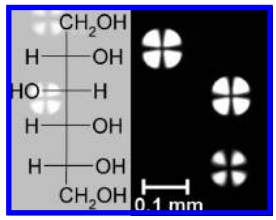

Figure 1. Chemical structure of D-sorbitol superimposed upon an optical micrograph of pure sorbitol spherulites viewed between crossed polarizers.

these considerations, is a thin section of a sphere in which chromophores are arranged uniaxially with respect to the radii. Every orientation can be evaluated in normal incidence eliminating the need for moving samples, moving optical components, and intensity corrections. Thus, we set out to further our study of the process of dyeing polycrystalline spherulites, a natural outgrowth of our work on dyeing single crystals[3] and spherulitic biopathological structures.[13] We show that the study of the LD of dyed spherulites beautifully illustrates the hard won principles of crystal optics[14] whose improper application have caused confusion with respect to the angular dependence of *A* and *T*.

Sorbitol Spherulites. Many polycrystalline substances organize themselves radially into so-called spherulites[15] including simple molecular crystals,[16] salts,[17] high polymers,[18] and proteins.[19] Radial crystalline aggregates of sorbitol, recently described by Yu,[20] are finely structured with the optical symmetry of a sphere (Figure 1). They are not easily distinguishable from the melt without polarizing elements (Figure 2c). With appropriate solutes, sorbitol spherulites are ideal for the analysis of the orientational dependence of LD.

The symmetry of flattened spherulites grown between a slide and coverslip and viewed between crossed polarizers is that of a circular disk displaying the 'Maltese cross' characteristic of organized radial bodies (Figure 1). Experimental details can be found in the Supporting Information.

The rotating polarizer technique[21] was used to make images of retardance (δ) in terms of the absolute value of the sine of this quantity (Figure 2a), the slow vibration direction which is parallel to the spherulite radii (Figure 2b), and the transmission (Figure 2c). The spherulites, when fully grown, display linear birefringence characterized by first order phase shifts, punctuated by a core with near-zero birefringence, a consequence of viewing a uniaxially radius end-on.

The spherulite texture, analyzed using atomic force microscopy (AFM), resembles that of fur, with fine overlaid fibrils 30 nm thick (see Supporting Information). The X-ray diffraction peaks of sorbitol spherulites are broader and weaker than the peaks of the common γ polymorph, indicative of a reduction in crystallinity and consistent with fine fibers. Even though spherulites are optically anisotropic, they cannot be assigned as a known polymorph.[22] Yu has designated this material "solidified melt I".[20]

Dyeing Spherulties: A General Method of Solute Alignment. Many laser dyes, textile dyes, biological stains, and NLO chromophores are soluble in molten sorbitol. When the spherulite crystallization front passes through the melt, the dyes are invariably oriented giving rise to highly dichroic disks. Figure 3 shows a montage of dichroic sorbitol spherulites containing a variety of chromophores listed in the caption. More than 50 colored compounds behaved in this way. Only one compound having appreciable solubility in sorbitol (methyl green) failed to show measurable anisotropic absorption. Orientation at the crystal growth front was a general phenomenon. The concentration of chromophores within spherulites is equal to that of the melt because diffusion at room temperature is much slower than crystal growth.

The common azo dye, amaranth (acid red 27, C.I.# 16185) is photostable and highly soluble in sorbitol, producing spherulites with strong LD at 532 nm (Figure 4). Absorbance measurements and automated imaging of the LD[23] confirm that the radial vibration direction is more absorbing.Figure 5.

Latitude vs Longitude. An oscillator organized in a section of a spherulite can be defined by two angles, θ and φ, that describe, respectively, the azimuth of the oscillator in the plane section and the inclination of the oscillator with respect to the unique axis. A θ rotation is parallel to the wave vector **k**. It follows a procession of radii along a line of latitude; a φ-rotation is perpendicular to **k**. It follows the inclination of oscillators from a pole to an equator along a line of longitude.

Spherulites containing amaranth were photographed (CCD camera) through a microscope using monochromatic (525 nm) linearly polarized radiation in order to obtain intensity (*I*) images. In addition to simultaneously imaging all possible orientations of the absorbance ellipsoid, these images provide the transmission of the melt, a valuable reference (Figure 6) and a convenient assay of the optical homogeneity of the film.

(9) Heavens, O. S. *Optical Properties of Thin Solid Films*; Buttersworth Scientific: London, 1955.
(10) Johannson, L. B.-Å *J. Phys. Chem.* **1978**, *82*, 2604–2609.
(11) Lopes, S.; Fernandes, M. X.; Prieto, M.; Castanho, M. A. R. B. *J. Phys. Chem. B* **2001**, *105*, 562–568.
(12) Nordén, B.; Lindblom, G.; Jonás, I. *J. Phys. Chem.* **1977**, *81*, 2086–2093.
(13) (a) Kurimoto, M.; Müller, B.; Kaminsky, W.; Kahr, B.; Jin, L.-W. *Mol. Cryst. Liq. Cryst.* **2002**, *389*, 1–9. (b) Jin, L.-W.; Claborn, K.; Kurimoto, M.; Sohraby, F.; Estrada, M.; Kaminsky, W.; Kahr, B. *Proc. Natl. Acad. Sci.* **2003**, *100*, 15294–15298. (c) Kahr, B.; Kaminksy, W.; Kaminsky, W.; Kahr, B.; Powell, S.; Jin, L.-W. *Micron* **2006**, *37*, 324–338.
(14) (a) Pancharatnam, S. *Proc. Ind. Acad. Sci. A* **1955**, *42*, 86–109. (b) Ramachandran, G. N.; Ramaseshan, S. in *Handbuch der Physik*; Springer-Verlag: Berlin, 1961; 1–217.
(15) Gránásy, L.; Pusztai, T.; Tegze, G.; Warren, J. A.; Douglas, J. F. *Phys. Rev. E* **2005**, *72*, 011605.
(16) (a) Bernauer, F. *Gedrillte krystalle*; Gebrüder Borntraeger: Berlin, 1929; (b) Contemporary researchers are few. See for example: Sadlik, B.; Talon, L.; Kawka, S.; Woods, R.; Bechhoefer, *J. Phys. Rev. E* **2005**, *71*, 061602; ref 20; Pisula, W.; Kastler, M.; Wasserfallen, D.; Pakula, T.; Müllen, K. *J. Am. Chem. Soc.* **2004**, *126*, 8074–8075; Lin, T.-F.; Ho, R.-M.; Sung, C.-H.; Hsu, C.-S. *Chem. Mater.* **2006**, *18*, 5510–5519.
(17) (a) Morse, H. W.; Warren, C. H.; Donnay, J. D. *Am. J. Sci.* **1932**, *223*, 421–439. (b) Morse, H. W.; Donnay, J. D. H. *Am. J. Sci.* **1932**, *223*, 440–461.
(18) Lotz, B.; Cheng, S. Z. D. *Polymer* **2005**, *46*, 577–610.
(19) (a) Krebs, M. R. H.; Bromley, E. H. C.; Rogers, S. S.; Donald, A. M. *Biophys. J.* **2005**, *88*, 2013–2021. (b) Heijna, M. C. R.; Theelen, M. J.; van Enckevort, W. J. P.; Vlieg, E. *J. Phys. Chem. B* **2007**, *111*, 1567–1573.
(20) (a) Yu, L. *Cryst. Growth Des.* **2003**, *3*, 967–971. (b) Yu, L. *J. Am. Chem. Soc.* **2003**, *125*, 6380–6381.
(21) Glazer, A. M.; Lewis, J. G.; Kaminsky, W. *Proc. R. Soc. London A* **1996**, *452*, 2751–2765.
(22) (a) Kim, H. S.; Jeffrey, G. A.; Rosenstein, R. D. *Acta Crystallogr.* **1971**, *B27*, 307–314. (b) Quinquenet, S; Ollivon, M.; Grabielle-Madelmont, C. *Thermochem. Acta* **1988**, *125*, 125–140. (c) Schouten, A.; Kanters, J. A.; Kroon, J.; Comini, S.; Looten, P.; Mathlouthi, M. *Carbohydr. Res.* **1998**, *312*, 131–137.
(23) Kaminsky, W.; Claborn, K.; Kahr, B. *Chem. Soc. Rev.* **2004**, *33*, 514–525.

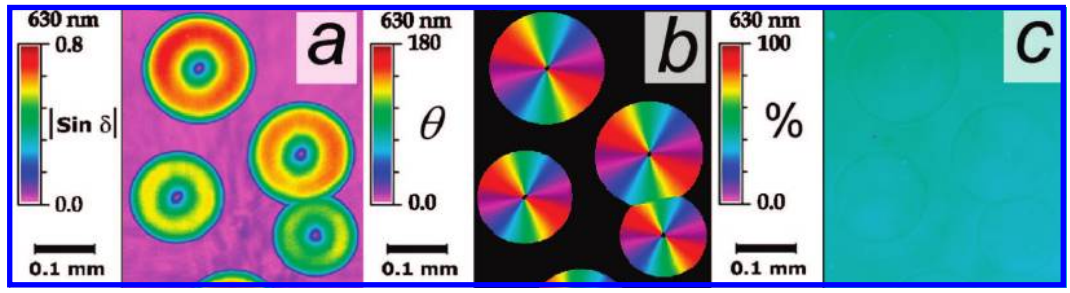

Figure 2. (a) False-color images of $|\sin \delta|$ ($\delta = (2\pi\Delta nL)/\lambda$, where Δn is the linear birefringence, L is the thickness, and λ is the wavelength of incident light), (b) orientation of the slow vibration direction (θ) in degrees counterclockwise from the horizontal, and (c) transmittance (T) in % of pure sorbitol spherulites.

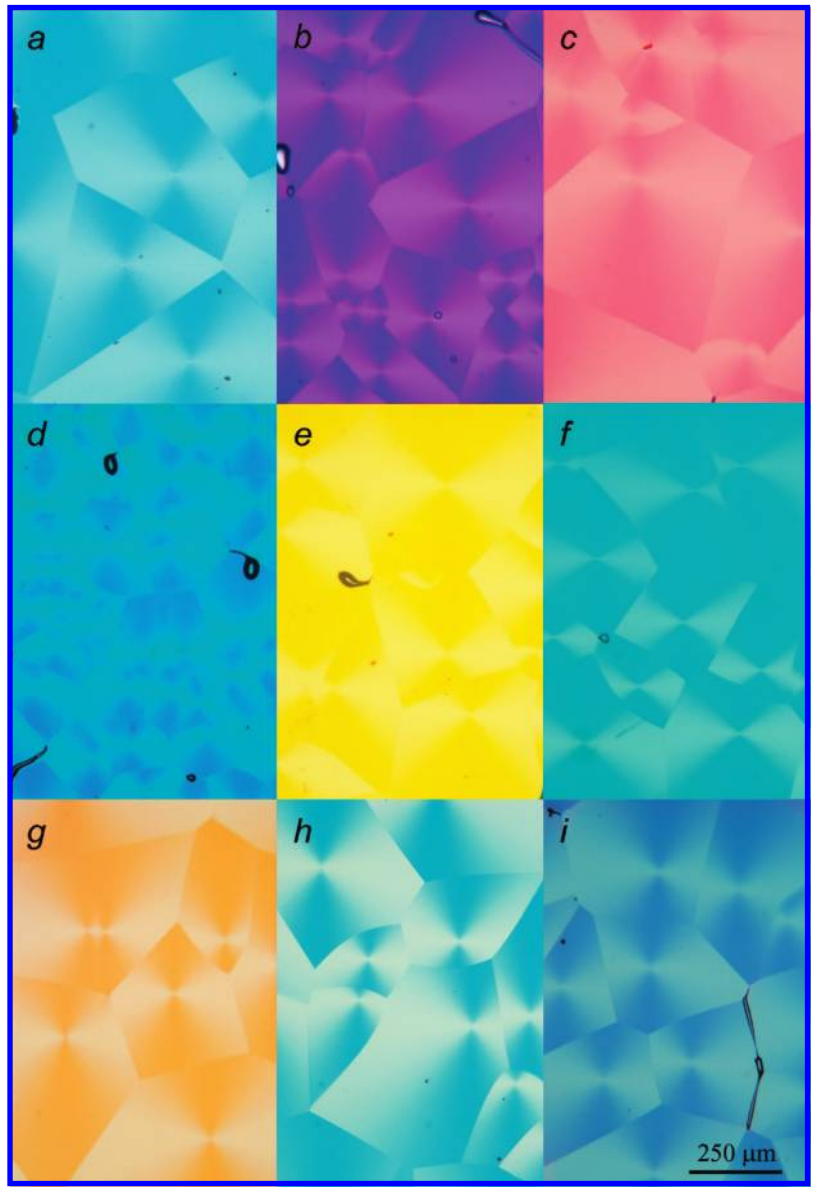

Figure 3. Montage of dyed sorbitol spherulites. 0.05 wt % (a) new methylene blue, CI# 52030, (b) pinacyanol chloride, CA# 2768-90-3 (c) amaranth, CI# 161185 (d) 0.1 wt % HIDCI, CAS# 36536-22-8 (e) 0.05 wt % acridine orange basic, CI# 46005:1 and (f) methylene blue, CI# 52015 (g) 0.1 wt % DAST, (h) 0.75 wt % Chicago sky blue 6B, CI# 24410 (i) 0.05 wt % sulfonanzo III.

In a θ rotation, the absorption ellipsoid is rotated about an axis parallel to **k** and typically involves either the rotation of the plane of polarization of the incident radiation or rotation of the sample. The radial variation of T inside and outside of the spherulite is obtained by analyzing concentric rings of radii r in normal incidence with a fixed polarizer. T was converted to A, and both sets of data were then fit to a $\cos^2 \theta$ function bounded by the data minima and maxima (Figure 7).

In a φ rotation, the absorption ellipsoid is rotated by an axis perpendicular to **k**. In anisotropic thin films, this requires

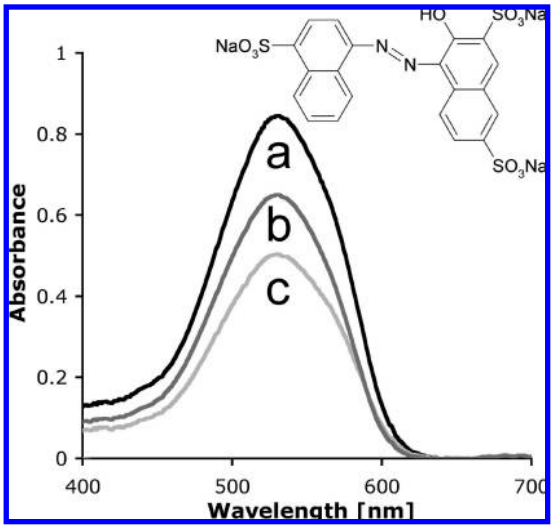

Figure 4. Absorption spectra of (b) the isotropic sorbitol melt containing 0.5 wt % amaranth (structure inset) with the plane of polarization along the (a) radial and (c) tangential directions of the spherulites

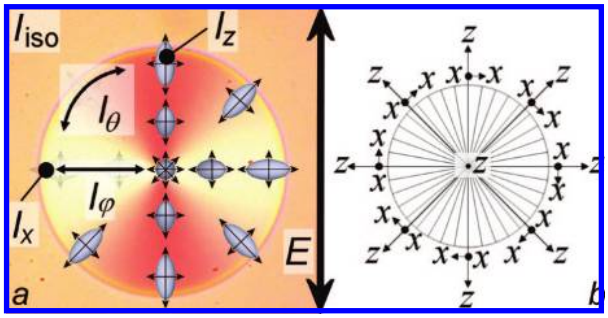

Figure 5. (a) Idealized uniaxial index/absorption ellipsoid sections superimposed upon a contrast-enhanced, polarized light micrograph of a spherulite containing 0.75 wt % amaranth. The arrows on the surface of the ellipsoids indicate the orientation of the vibration directions in the specified domain; the lengths of the arrows qualitatively represent the magnitude of the absorption coefficient of the vibration direction. The plane of polarization of the electric vector of the incident radiation is indicated by the heavy vertical double arrow. (b) Specified directions in an idealized spherulite.

inclining the sample with respect to the incident radiation. For measurements in single crystals, each unique φ rotation requires the preparation of a new plane-parallel slice. In a spherulite, φ rotations are realized by moving from the center where the z direction of the ellipse is parallel to **k** to the edge of the spherulite along a radius where z is perpendicular to **k**. φ rotations uncomplicated by θ are assessed in a linearly polarized T image of a spherulite along the principal diameters ($\varphi_\perp$ and $\varphi_\parallel$ Figures 6a and 8).

Discussion

Standard works express the probability of a spectroscopic transition in terms of the square of the projection of the transition moment describing that excitation onto the electric field vector of the incoming light.[2] However, the electric field vibrations in a dielectric anisotropic medium are constrained by the index and absorption ellipsoids of the medium, and thus the quantity $|M \cdot E|^2$ where M is the transition moment and E is the electric field of the incident light, cannot be assessed directly by arbitrary rotations of the sample. Failure to recognize the constraints of the indicatrix is undoubtedly the source of the cited confusion.[1,24]

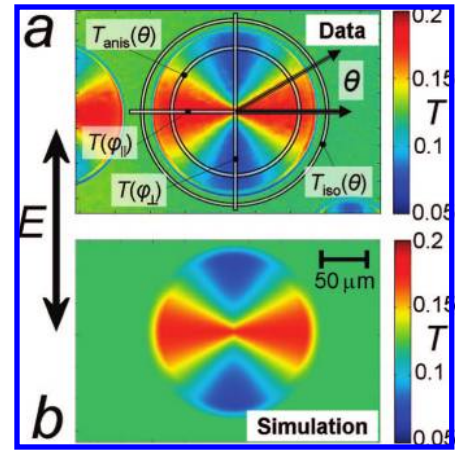

Figure 6. (a) Transmittance of a spherulite containing 0.75 wt % amaranth. θ rotations of the absorption ellipsoid are measured by analyzing concentric rings of data with respect to vertically polarized radiation E at a distance r from the center of the spherulite. Two unique rotations, $\varphi_\perp$ and $\varphi_\parallel$ are measured by analyzing orthogonal diameters parallel and perpendicular to the applied polarization. (b) Simulated transmittance.

At low optical densities, eqs 1 and 2 describe the transmitted intensity of light propagating through an absorbing medium equally well with respect to a θ rotation. As the optical density is increased, the accuracy of two models diverges (Figure 7). T follows a $\cos^2\theta$ dependence, not A.

At some angle, θ_{eq}, the optical density of the spherulite must be equal to that of the melt. $A^{iso} = A^{anis}(\theta_{eq})$; $T^{iso} = T^{anis}(\theta_{eq})$. Presuming z is the unique axis, the extinction coefficients in a uniaxial anisotropic domain are related to the isotropic extinction coefficient by

$$\varepsilon^{iso} = \frac{2\varepsilon_x^{anis} + \varepsilon_z^{anis}}{3} \tag{3}$$

Because path length and concentration are constant in spherulite sections, eq 3 becomes

$$A^{iso} = \frac{2A_x^{anis} + A_z^{anis}}{3} \tag{4}$$

Together, eqs 1 and 4 predicts an invariant θ_{eq} when the fibril is 54.7° (the magic angle) from E. Together, eqs 2 and 4 expressed in terms of T become

$$\theta_{eq} = \arccos\sqrt{\frac{((T_x^{anis})^2 \times T_z^{anis})^{\frac{1}{3}} - T_z^{anis}}{T_x^{anis} - T_z^{anis}}} \tag{5}$$

derived in the Supporting Information.

This expression predicts that θ_{eq} will decrease from 54.7° as either the optical density or anisotropy increases. In the optically thin sample, $T(\theta)_{eq}$ was 53° from the plane of polarization (Figure 7); eq 5 predicts 53.6°. In the optically thick sample, θ_{eq} was 44° from x (Figure 7); eq 5 predicts 45.8°. θ_{eq} from A theory is an adequate approximation only in the former case.

Equation 2 correctly describes θ rotations as these do not change the projection of the index ellipsoid with respect to the wave vector of the light. In a θ rotation, the absorption

(24) Libowitzky, E.; Rossman, G. R. *Phys. Chem. Miner.* **1996**, *23*, 319–327.

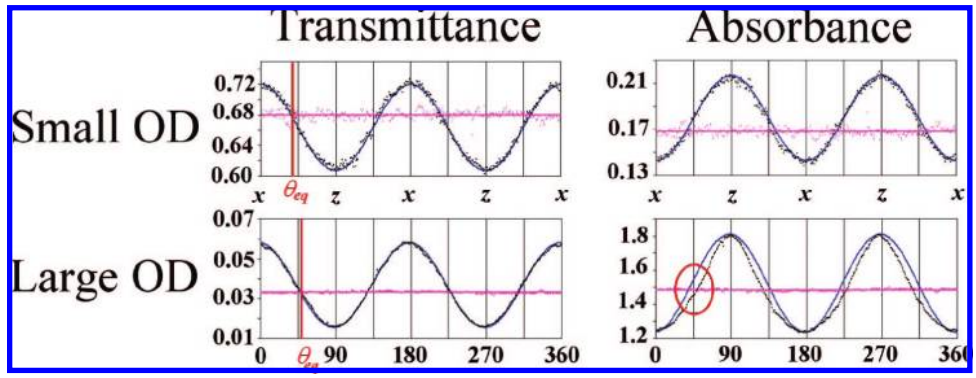

Figure 7. Transmittance (left column) and the corresponding absorbance (right column) plots from spherulites that are optically thin (0.1 wt % amaranth, upper row) and optically thick (1.0 wt % amaranth, lower row). The solid pink line represents the average value of the isotropic data (pink dots). The solid blue line is a $\cos^2\theta$ fit of the data from the anisotropic spherulitic domain (black dots). The vertical red line in the transmittance curves indicates the measured equivalence point. In the optically thick sample θ_{eq} has shifted toward z. The discrepancy between the absorbance $\cos^2\theta$ model and the measured equivalence point is circled in red in the graph on the lower right.

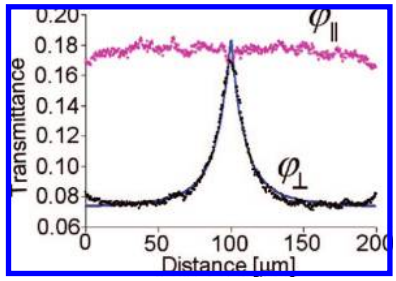

Figure 8. Transmittance for a $\varphi_\perp$ rotation (black points) and for a $\varphi_\parallel$ rotation (pink points) in a spherulite containing 0.75 wt % amaranth. The solid blue line is a fit to eq 10. Slight divergences at the extrema are due to spherulite curvature at the edges. As can be seen in Figure 6b, the edges are least well simulated.

coefficients of the two vibration directions remain constant; only the *intensity* of the light that is projected onto the vibration directions (x,z) changes, not the angle between E and M. Equation 2 in terms of absorbance and absorption coefficients

$$T(\theta) = 10^{-A_x}\cos^2\theta + 10^{-A_z}\sin^2\theta \tag{6}$$

$$T(\theta) = 10^{-\varepsilon_x \cdot c \cdot l}\cos^2\theta + 10^{-\varepsilon_z \cdot c \cdot l}\sin^2\theta \tag{7}$$

φ rotations do, however, change the cross-section of the absorption/index ellipsoids with respect to the wave vector of the light. In a spherulite, any φ rotation will change the absorption coefficient of the vibration directions parallel to the radial direction; the tangential vibration direction has a constant coefficient. Because φ rotations progressively change the angle between E and M, eq 1 is the appropriate functional dependence. Equation 1 in terms of molar extinction coefficients is

$$\varepsilon(\phi) = \varepsilon_z\cos^2\phi + \varepsilon_x\sin^2\phi \tag{8}$$

The transmittance for a φ rotation is expressed as

$$T(\phi) = 10^{-((\varepsilon_z\cos^2\phi + \varepsilon_x\sin^2\phi)\cdot c \cdot l)} \tag{9}$$

and can be rearranged to give

$$T(\phi) = 10^{-((\varepsilon_z + (\Delta\varepsilon)\cos^2\phi)\cdot c \cdot l)} \text{ where } \Delta\varepsilon = \varepsilon_z - \varepsilon_x \tag{10}$$

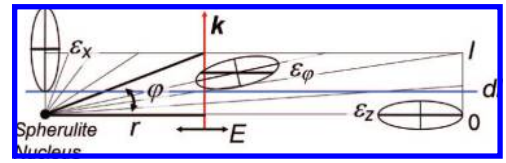

Figure 9. Schematic representation viewed parallel to a φ rotation axis for a sample of thickness l. The cross-sections of the ellipsoid for various rotations are indicated. An infinitesimally thin slice, dl, is indicated by the blue line. Light propagating through the sample a distance r from the center will encounter a continuous distribution of ellipsoids between φ and 0°.

φ describes the pitch of the ellipsoid for a spherulite nucleating on the substrate, as shown in Figure 9, and is related to r, the distance from the center of spherulite by $\tan\varphi = l/r$.

Integrating eq 10 over an infinitesimally thin slice yields,

$$T(\phi) = 10^{-\int_0^l [\varepsilon_x + (\Delta\varepsilon)\cos^2(\phi)]\cdot c\ dl} \tag{11}$$

$$T(r) = 10^{-\int_0^l [\varepsilon_x + (\Delta\varepsilon)\cos^2(\tan^{-1}(l/r))]\cdot c\ dl} \tag{12}$$

$$T(r) = 10^{-\varepsilon_x \cdot c \cdot l + (-\Delta\varepsilon \cdot c \cdot r\ \tan^{-1}(l/r))} \tag{13}$$

or

$$T(r) = e^{-\alpha_x \cdot l + (-\Delta\alpha \cdot r\ \tan^{-1}(l/r))} \tag{14}$$

where $\alpha \approx 2.303\varepsilon c$ (cm^{-1}). Figure 8 shows the $\varphi_\perp$ rotation data fit to eq 14.

The transmittance for any point on a spherulite is completely described by combining expressions 5 and 6 derived from the analysis of θ and φ rotations:

$$T(\theta,\phi) = e^{-\alpha(\phi_\parallel)}\cos^2\theta + e^{-\alpha(\phi_\perp)}\sin^2\theta \tag{15}$$

Expressed in terms of r,

$$T(\theta,r) = e^{-\alpha_x \cdot l}\cos^2\theta + e^{-(\alpha_z\cos^2\phi + \alpha_x\sin^2\phi)l}\sin^2\theta \tag{16}$$

or

$$T(\theta,r) = e^{-\alpha_x \cdot l}\cos^2\theta + e^{-\alpha_x \cdot l + (-\Delta\alpha \cdot r\ \tan^{-1}(l/r))}\sin^2\theta \tag{17}$$

Figure 6b was simulated within eq 17. The details within the Stokes−Mueller formulation can be found in the Supporting Information.

Conclusion

In evaluating the angular dependence of LD in an anisotropic medium, one must determine how the optical indicatrix con-

strains the vibrations of the electric field of incident electromagnetic radiation. If an anisotropic substance were nothing more than a body with unequal absorption coefficients, eq 2 would always hold. However, even when a material contains nothing more than oscillators embedded in an otherwise isotropic medium, vibration directions are established in a plane perpendicular to the wave vector along and perpendicular to the principal absorbing direction.[14] This has the effect of giving distinct physical interpretations to θ and φ rotations; in the former case, $|E \cdot M|^2$ cannot be evaluated directly if all that is known is the orientation of the plane of incident polarization. While other dye-doped spheres are known in the form of micelles and liposomes, these tend to be small, labile, and by nature difficult to constrain to a plane. Doped sorbitol spherulites, on the other hand, are easily prepared and thus with contemporary camera technology, their analysis serves as an experimental tutorial on the principles anisotropic absorption that have otherwise been confused in the literature.

Acknowledgment. B.K. thanks the National Science Foundation for support of this research. We are most grateful for helpful discussions with Professors Werner Kaminsky, and Dor Ben-Amotz, as well as for the contributions of Matthew Nichols. Dr. Ryan Sours is acknowledged for his contribution of the AFM images in the Supporting Information.

Supporting Information Available: Experimental section, details of simulations of Figure 6b, atomic force micrographs, and derivation of equivalence point. This material is available free of charge via the Internet at http://pubs.acs.org.

JA802322T